IET Journals

The Institution of Engineering and Technology

Active and reactive power control of wind farm for enhancement transient stability of multi-machine power system using UIPC

Mehdi Firouzi[1] ✉, Gevork B. Gharehpetian[2], Younes Salami[3]

[1]*Department of Electrical Engineering, Abhar Branch, Islamic Azad University, Abhar, Iran*
[2]*Electrical Engineering Department, Amirkabir University of Technology, Tehran, Iran*
[3]*Department of Electrical and Computer Engineering, Faculty of Engineering and Applied Science, Memorial University, St. John's, NL, Canada*
✉ *E-mail: paper_mehdi12@yahoo.com*

Abstract: This study discusses the connection of wind farms (WFs) to power system through unified inter-phase power controller (UIPC) for enhanced transient stability of the power system. The power circuit of the UIPC is based on the conventional inter-phase power controller (IPC), which its phase-shifting transforms are substituted by two series converters and one shunt converter. During fault condition, the WF connected through UIPC acts as STATCOM with capability of the active and reactive power control at UIPC connecting point. Based on the UIPC model and low-voltage ride-through requirements of the new grid codes, a control system for active and reactive powers control is proposed for enhancement transient stability of power system. The proposed approach is validated in a four-machine two-area test system. Power systems computer aided design (PSCAD)/EMTDC simulation results demonstrate that the UIPC provides an effective solution for enhancement of transient stability of power system including WFs.

1 Introduction

As the integration level of wind farms (WFs) is increasing, concerns regarding the stability of power system are becoming more and more important. Wind turbines (WTs) technologies utilised in WFs can be classified into fixed speed wind turbine (FSWT) and variable speed wind turbine (VSWT) [1, 2]. Despite current trend is towards the use of VSWTs due to their high efficiency, many FSWTs have been installed and utilised in WFs in some countries especially in Iran. FSWT-based WFs utilises inexpensive squirrel cage induction generator (SCIG) directly connected to the grid. The utilisation of the SCIG in WFs reduces the cost of installation and maintenance due to their simple and robust construction [2, 3]. However, they cannot control active and reactive power, which causes negative impacts on power system stability during fault condition [3, 4]. Due to integration of WFs to power system, the total active power generation is sum of the conventional synchronous generator (SG) and WFs output powers. Therefore, the active power variations of SGs can be affected by controlling the WF output power and vice versa during fault. Also, the transmission system operators have elaborated specific technical requirements for the integration of WFs to power system as low-voltage ride-through (LVRT) capability [4]. These requirements specify that large WFs connected to power system, must withstand voltage sags and have to provide the reactive power compensation (RPC) to support the connection point (CP) voltage to assist power system stability during system disturbance.

Therefore, controlling the injected active and reactive power of WFs can improve transient stability of power system. Meet these requirements involve the fact that WFs will be able to control active and reactive power during system disturbance which it does not have at fixed speed. Therefore, it requires the installation of additional equipment for this purpose. Flexible AC transmission system (FACTS) controllers based on voltage source converters (VSCs) provide an effective solution to control power flow, voltage and transient stability, in addition improvement of LVRT capability [5–9]. In [5], a hierarchical scheme has been suggested for coordinated control of FACTS controllers and power system including WFs, to provide power flow control and enhance transient stability of interconnected power system. The application of shunt FACTS controllers such as STATCOM and SVC to

provide RPC are the well-known solution proposed to improve voltage regulation and transient stability of power system including WFs [6, 7]. In [8], the application of STATCOM and battery energy storage (BES) on a multi-machine system with a WF to provide voltage regulation and transient stability of power system has been investigated. The simulations results demonstrate that the integration of STATCOM and BES is more effective than the STATCOM alone for transient stability of power system.

In [9], the application of static synchronous series compensator for power flow control and stability enhancement of a offshore WF connected to a one-machine infinite bus system have been suggested. In [10], the application of dynamic voltage restorer has been proposed to improve stability of power system including SCIG-based WF. In [11, 12], the bridge-type fault current limiter with discharging resistor has been used for transient stability enhancement of FSWT-based WF during fault condition.

In this paper, the application of unified inter-phase power controller (UIPC) [13] and a unified control scheme including active and reactive power control is proposed to improve the transient stability of power system including SCIG-based WF. The UIPC is based on conventional inter-phase power controller (IPC), which has capability of voltage isolation, short circuit current limitation and power flow control [14, 15]. It includes two series converters (SECs) and a shunt converter (SHC) connected by a common DC-link capacitor. The WF connected through UIPC acts as STACOM with capability of active and reactive power injection at CP to power system during fault condition. The UIPC model is developed based on phase angels of injected SECs voltage to design the proposed control scheme. The control scheme of the UIPC includes active and reactive power control loops. The reactive power loop provides reactive power to restore the CP voltage in compliance with LVRT specifications. The active power loop control transmits the active power generated by WF to power system. In addition, a modified control scheme is implemented in the active power control loop to improve transient stability of power system. The classic two-area four-machine system and PSCAD/EMTDC software are used for this study. PSCAD/EMTDC simulation results show that the UIPC provides an effective means for improvement of the transient stability of the power system including WFs.
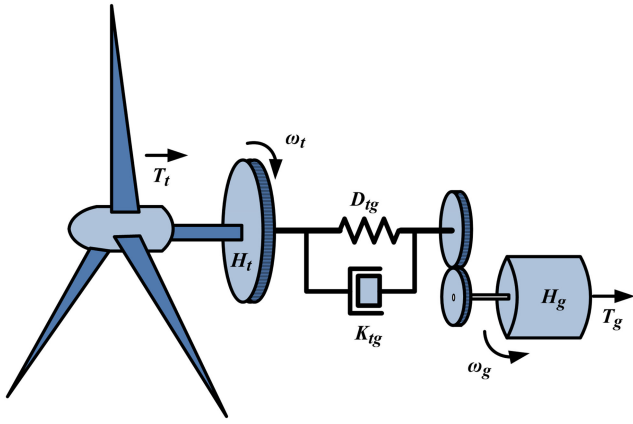
IET Renew. Power Gener., 2017, Vol. 11 Iss. 8, pp. 1246-1252

1246

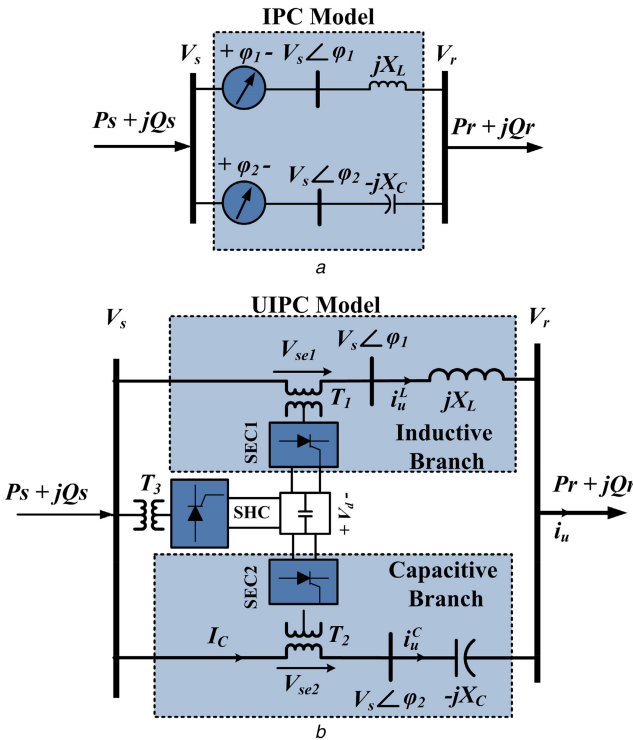**Fig. 1** *Drive train system*

Fig. 2 *Single line diagram of*
(a) the conventional IPC, *(b)* the UIPC model

2 Wind farm model

The WF is represented by an equivalent aggregated SCIG driven by an aggregated FSWT through an aggregated gearbox. As a result, the rating of the equivalent WT is the sum of the rating of all the individual WTs with the same equations, mechanical and electrical parameters in per unit, and also similar control parameters [16]. The PSCAD/EMTDC software library provides a standard model for the SCIG, represented by a standard seventh-order model in a d–q reference frame, which is also used in this paper.

2.1 Wind turbine model

In general, the mechanical torque obtained from the wind can be described, as follows [17, 18]:

$$T_t = \frac{0.5 A_w C_p(\lambda, \beta) v_w^3}{\omega_r} \quad (1)$$

where T_t is the torque extracted from the wind, ρ is the air density, v_w is the wind speed, $A_w = \pi R^2$ is the area covered by the WT rotor and R is the radius of the tip speed ratio, ω_r is the angular

mechanical speed and $C_P(\beta, \lambda)$ is the power coefficient as function of the tip speed ratio (λ) and pitch angle (β).

2.2 Drive train model

The drive train of a WT in general consists of a blade pitch system with hub and blades, rotor shaft, gear box and generator as shown in Fig. 1. It is described by two-mass model and written as follows:

$$\frac{d\omega_g}{dt} = \frac{1}{2H_g}(-T_g + K_{tg}(\delta_t - \delta_g) - D_{tg}(\omega_t - \omega_g)) \quad (2)$$

$$\frac{d\delta_{tg}}{dt} = (\omega_t - \omega_g) \quad (3)$$

$$\frac{d\omega_t}{dt} = \frac{1}{2H_t}(T_t - K_{tg}(\delta_t - \delta_g) - D_{tg}(\omega_t - \omega_g)) \quad (4)$$

where T_t and T_g are the mechanical and electromagnetic torque, respectively. H_t and H_g are the equivalent turbine-blade and generator inertia, respectively. ω_t and ω_g are the turbine and the generator angular speed, respectively. K_{tg}, D_{tg} and δ_{tg} are the shaft stiffness, damping constant and angular displacement between two ends of the shaft, respectively [17].

2.3 Pitch angle control

The MOD2 type pitch angle control is considered in this study using PSCAD/EMTDC software library. It is controlled to optimise the error signal of output power of induction generator (P_r) and reference value (P_{r_ref}) through proportional-integral (PI) controller [18].

3 UIPC operation

Fig. 2a shows the power circuit of the conventional IPC. It should be emphasised that this device is fully different from inter-phase power flow controller. It consists of two parallel branches including capacitive and inductive reactance in series with the phase shifting transformers (PSTs). It is capable of power flow control, short circuit current limitation and voltage isolation [13–19]. However, the capabilities of the IPC are limited due to the phase-shift limitation of PSTs. In [13], the UIPC is proposed to overcome IPC limitations. It consists of two SECs instead of PSTs and an SHC. All converters are connected to a common DC-link capacitor as shown in Fig. 2b.

The SECs of the UIPC shift the phase angle of the UIPC bus (V_S) by injecting series voltages with adjustable magnitude and phase angle in each branch (V_{se1} and V_{se2}) as shown in Fig. 2b. By using this figure, the magnitude and the phase of voltages V_{se1} and V_{se2} are expressed by the following equations:

$$|V_{sei}| = \frac{1}{2} V_s \sin(\varphi_i), \quad i = 1, 2 \quad (5)$$

$$\theta_{sei} = \theta_s - \varphi_i + \frac{\pi}{2}, \quad i = 1, 2 \quad (6)$$

The SHC of the UIPC controls the UIPC bus voltage and DC-link voltage to provide active power exchange with other two SECs. The reactor and capacitor of inductive and capacitive branches should be equal ($X_C = X_L = X$) and tuned at the fundamental frequency [13–19].

3.1 UIPC model

Fig. 3 shows the equivalent circuit of the UIPC. As seen in this figure, the equivalent circuit of the UIPC includes series equivalent circuit (SEEC) and shunt equivalent circuit. The losses of the transformers are modelled by R_{se} and VSCs are modelled by R_{sh}. Considering the losses of VSCs and transformers, the active power
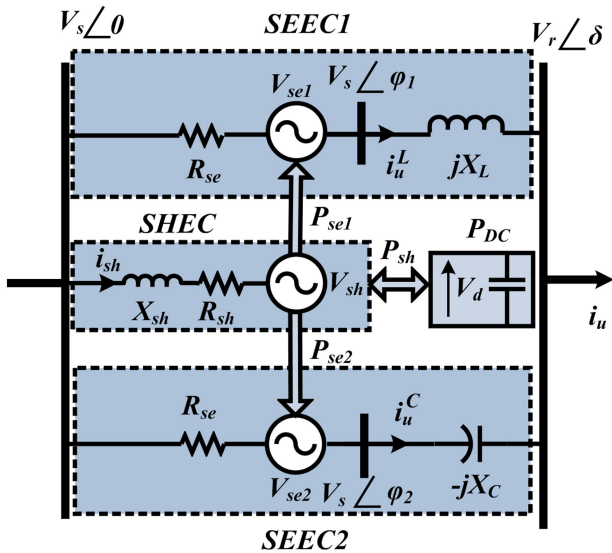
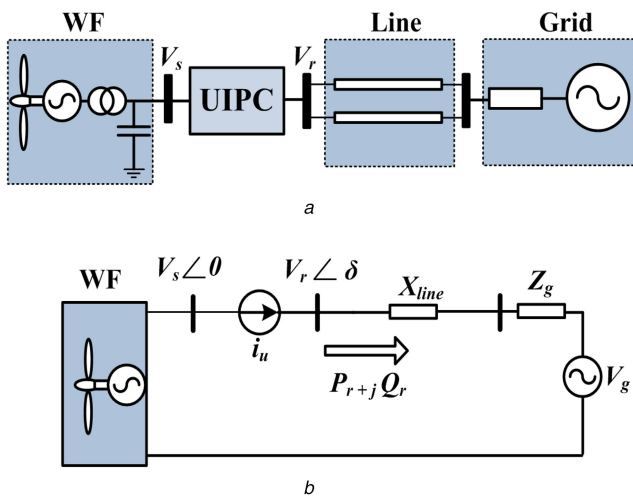**Fig. 3** *Equivalent circuit of UIPC*

Fig. 4 *WF connected to power system*
(a) Power system with UIPC, *(b)* Equivalent circuit of system with UIPC

exchange between the UIPC SECs and SHC can be written as follows:

$$P_{se1} + P_{se2} + P_{sh} = 0 \tag{7}$$

where P_{se1}, P_{se2} and P_{sh} are the active power exchange between the SECs and SHC of the UIPC and DC link, respectively. They can be written as follows:

$$
\begin{aligned}
P_{se1} &= \mathrm{Re}\left[V_{se1} i_u^L + R_{se} i_u^{L^2}\right] \\
P_{se2} &= \mathrm{Re}\left[V_{se2} i_u^C + R_{se} i_u^{C^2}\right] \\
P_{sh} &= \mathrm{Re}\left[V_{sh} i_{sh} + R_{sh} i_{sh}^2\right]
\end{aligned}
\tag{8}
$$

Considering Fig. 3, the SEECs current of the UIPC (i_u^L and i_u^C) can be written as follows:

$$i_u = i_u^L + i_u^C = \frac{V_S \angle \varphi_1 - V_r \angle \delta}{jX_L} + \frac{V_S \angle \varphi_2 - V_r \angle \delta}{-jX_C} \tag{9}$$

By substituting $X_L = X_C = X$, (14) can be written as follows:

$$i_u = \frac{V_S \angle \varphi_1 - V_r \angle \delta}{jX} + \frac{V_S \angle \varphi_2 - V_r \angle \delta}{-jX} \tag{10}$$

Rewriting this equation results in the following equation:

$$i_u = \frac{V_S}{X} \sin(\alpha) \angle \beta \tag{11}$$

where $\alpha = (\varphi_2 - \varphi_1)/2$ and $\beta = (\varphi_2 + \varphi_1)/2$. Therefore, UIPC is modelled as current source based on the phase angles of injected series converter (SEC) voltage (i.e. φ_1 and φ_2).

3.2 Normal operation mode

Direct connecting of WFs to power system has two main disadvantages, uncontrollable active and reactive power flow and impact of power system condition on operation of WF. Connecting WFs to power system through UIPC provides controllable power flow and isolates the WF from power system. The normal function of the UIPC is control of the active power generated by WF and injected to the power system. Also, the UIPC controls the reactive power to maintain the acceptable power factor at bus, connecting the UIPC to the power system.

To study the effect of the UIPC on the performance of the WF under normal and fault conditions, the simplified schematic diagram of the WF connected to power system, shown in Fig. 4*a*, is used. Fig. 4*b* shows the equivalent circuit of the power system under normal operation mode. The grid is represented by the thevenin voltage (V_g) and impedance (Z_g). The UIPC is represented by (i_u). Using this figure, the apparent power transmitted from WF to power system (S_r) by UIPC can be determined as follows:

$$S_r = P_r + jQ_r = V_r * i_u^* \tag{12}$$

where $V_r = V_r \angle \delta$ is the CP voltage. Considering (11), P_r and Q_r are active and reactive powers transmitted from WF to power system by UIPC and can be written as follows:

$$P_r = 2\frac{|V_r||V_S|}{X}\sin(\alpha)\cos(\delta + \beta) \tag{13}$$

$$Q_r = 2\frac{|V_r||V_S|}{X}\sin(\alpha)\sin(\delta + \beta) \tag{14}$$

Using (13) and (14), the following equations can be derived:

$$S_r = \sqrt{P_r^2 + Q_r^2} = 2\frac{|V_r||V_S|}{X}\sin(\alpha) \tag{15}$$

$$\frac{Q_r}{P_r} = \tan(\delta + \beta) \tag{16}$$

Equations (15) and (16) show that apparent power of WF and ratio of reactive power to active power depend on the difference and sum of phase angles of SECs voltage, i.e. α and β, respectively. Fig. 5*a* presents the block diagram of the control system of UIPC SECs during normal conditions to control power flow of WF. The SHC of the UIPC controls the UIPC bus voltage and DC-link voltage to provide active power exchange with other two SECs during normal operation mode. The UIPC bus and DC-link voltage control can be achieved by controlling m_{sh} and φ_{sh}, respectively, in pulse width modulation (PWM) controller of the shunt converter as shown in Fig. 5*b*.

3.3 Fault operation mode

Fig. 6*a* shows the operating point of the UIPC current considering (11). As shown in this figure, the UIPC current is decomposed in two components as follows:
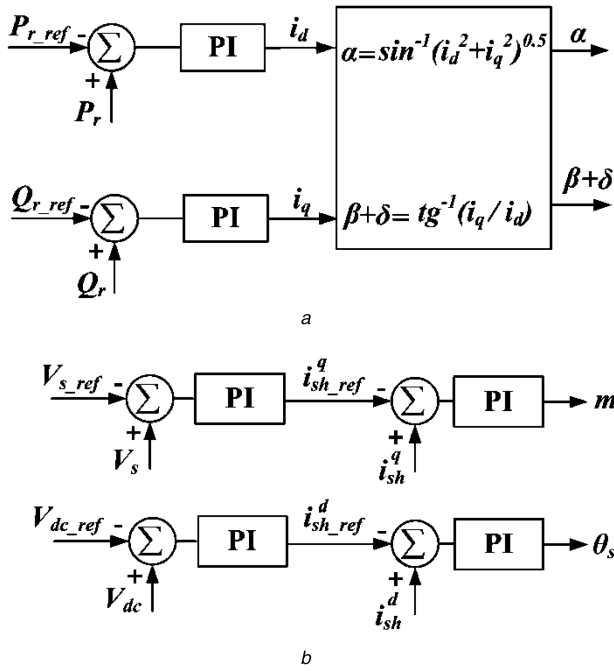
$$i_u = i_u^d + j i_u^q \tag{17}$$

Fig. 5 *Control system of UIPC during normal operation mode*
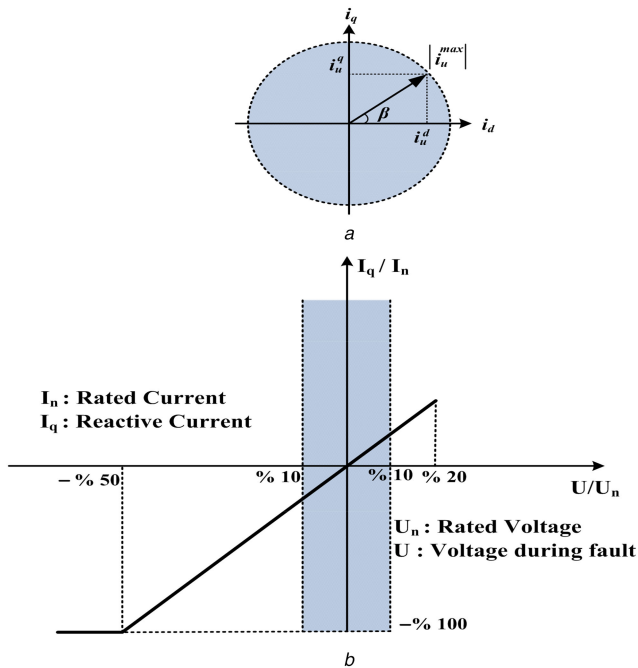*(a)* SECs of UIPC, *(b)* SHC of UIPC

Fig. 6 *Operating point and component of the UIPC*
(a) Locus of UIPC current, *(b)* Reactive current to be delivered to grid

i_u^d and i_u^q are the active and reactive components of the UIPC current. As shown in this figure, the amplitude of the UIPC current is controlled by α and the operating point (i.e. the active and reactive current of the UIPC) can be controlled by β. The new grid codes require WFs not only to stay connected to the power system but also to provide the reactive current compensation to support the CP voltage during fault as shown in Fig. 6*b* [4].

Therefore, the i_u^q should be controlled to provide the reactive current compensation to support the CP voltage during fault according to LVRT requirements. The range of the reactive current supported by the UIPC at the grid connection bus is limited by the maximum current rating of the UIPC SECs. Considering Fig. 6*b*, the reactive component of the UIPC current to provide reactive current compensation can be written as follows:

$$i_u^q = \begin{cases} \dfrac{2i_u^{max}(V_r - 0.5)}{V_r} & \text{if } |V_r| \geq 0.5\,\text{p.u.} \\ i_u^{max} & \text{if } |V_r| \leq 0.5\,\text{p.u.} \end{cases} \qquad (18)$$

where V_r is the rms of the rated CP voltage and i_u^{max} is the maximum current rating of the UIPC SECs. Also, the remaining current carrying capacity of the UIPC is used for active current as follows:

$$i_u^d = \sqrt{i_u^{max2} - i_u^{q2}} \qquad (19)$$

Fig. 7*a* shows the active and reactive currents injected by the UIPC to the grid during fault according LVRT requirements of E.ON grid code. The active and reactive component current of the UIPC (i.e. i_u^d and i_u^q) results in the active and reactive power exchange between the UIPC and line during the fault as shown in Fig. 7*b*.

3.4 Additional damping controller

Due to the high penetration of the WFs to power system, the total power generated is sum of the nearby SGs and WFs. So a change in the power generated of the WF causes changes of the output power and frequency of SGs. Now, if the active power generated of the WF controls in such a way that the changes of output power and frequency of SGs get reduced then this will cause enhancement in the transient stability.

Considering this background, in order to improve the stability of SGs of power system, additional damping control system integrated to active power control system of the UIPC. It includes a conventional P controller with a lead-lag compensator and a high-pass filter (HPF) by following equation:

$$\Delta P_r = K_u \left(\frac{sT_w}{1 + sT_w}\right)\left(\frac{1 + sT_1}{1 + sT_2}\right)\left(\frac{1 + sT_3}{1 + sT_4}\right)\Delta f_r \qquad (20)$$

where ΔP_r and Δf_r are input and output signals, respectively. K_u is controller gain, T_w is washout time constant, and T_1–T_4 are lead-lag time constants. The input and location of control signal are two main parameters for the controller. The UIPC CP to power system is selected as location of control system to avoid filtering the effect of transformers between power system and WF. Also, the frequency of the UIPC CP (f_r) is considered as the control signal to provide adequate information about oscillation modes. The UIPC CP frequency (f_r) passes through HPF, and then, the phase lag between f_r and P_r is compensated by lead-lag controller. The parameters of the lead-lag compensator are calculated based on the required compensation. Then, it passes through a P controller (K_u) and is added to the UIPC active power. The amount of damping is determined by K_u. Parameters of the proposed damping controller are given as follows:

$$\Delta P_r = 56\left(\frac{4.5s}{1 + 4.5s}\right)\left(\frac{1 + 0.15s}{1 + 1.2s}\right)\left(\frac{1 + 0.15s}{1 + 1.2s}\right)\Delta f_r \qquad (21)$$

3.5 Modification the UIPC control during fault operation mode

Fig. 8 shows the modified control block diagram of the UIPC during fault operation mode. It consists of two active and reactive power control loops. The reactive power control loop of the UIPC provides reactive current based on (18) to restore the CP voltage to satisfy LVRT requirements. The active power control loop of the UIPC controls active power of WF injected to power system. During grid fault, the active power transmitted from WF to power system by UIPC should be reduced to restore the power balance. To fulfil this objective, a control system as 'active power reduction-dependent current' is proposed, which depending on the i_u^d, reduces the active power reference (P_{r_ref}). Also, an additional damping control based on (21) is proposed and integrated to active power control loop system of the UIPC to damp the output power oscillation of nearby SGs after fault clearance.

4 Simulation results

Fig. 9 shows the single line diagram of the IEEE benchmark four-machine, two-area test system with UIPC. The parameters of this system are given in [20], and all generators (G1–G4) are equipped with power system stabiliser. It is assumed that an aggregated WF model consisting 50 SCIG-based WTs (50×2 MW) is connected to bus 6 of the power system as CP through UIPC. Three-phase short circuit fault is simulated at line 3 (L_3), which starts at $t = 10$ s. After 0.15 s, the circuit breaker isolates the faulted line. The parameters of this system are listed in the Appendix. The simulations are carried out for normal and fault operation modes of following cases:

- *Case A:* Connection through UIPC with modified control,
- *Case B:* Connection through UIPC without modified control,
- *Case C:* Direct connection to grid without using any UIPC.

Fig. 10a shows the rms value of the CP (bus 6) voltage for three cases. It can be observed that UIPC not only decreases the voltage drop of CP during fault but also it is quickly restored after fault clearance by RPC in case A. Fig. 10b shows the rotor speed of the SCIG for three cases. As shown in this figure, the SCIG rotor-speed swing is effectively damped in case A. Figs. 10c and d show
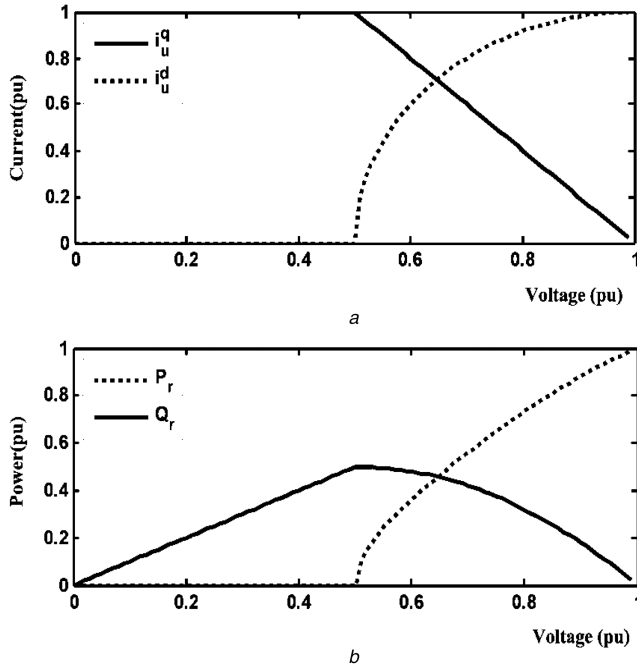
the total active and reactive power of the WF for three cases. As shown in Fig. 10c, during the fault period, the reactive power generated by the UIPC increases to 0.8 p.u. to support the CP voltage and help a fast recovery. As shown in Fig. 10d, during the fault period, the active power generated by the WF decreases to 0.5 p.u. and quickly reaches to pre-fault value by using the UIPC in case A.

Figs. 11a and b show the output power and rotor speed of G1. As shown in this figure, the output power oscillation and rotor speed variations are effectively reduced in case A by adding modified control system. Figs. 11c and d show the output power and rotor speed of G2. It can be seen that the output power and rotor speed variations of G2 are effectively reduced in case A by adding modified control system.

5 Conclusion

In this paper, the application of the UIPC for connecting FSWT-based WF to power system has been proposed. The operation of the UIPC is divided into normal and fault operation modes. The UIPC model based on injected SECs voltage of the UIPC has been developed to design the control scheme of the UIPC for normal and fault operation modes. In fault operation mode, a unified control scheme has been proposed for enhancement transient stability of power system. The unified control scheme of the UIPC includes active and reactive power control loops. The reactive power loop provides reactive power to restore the CP voltage in compliance with LVRT specifications. The active power loop control transmits the active power generated by WF to power system. Also, a modified control scheme has been added to active power control mode of UIPC to enhance power system transient stability. Based on the analytical studies and simulation results of the UIPC and proposed control scheme, the following points can be drawn:

- During fault operation mode, the UIPC acts like an STATCOM connected to power system, which can inject active and reactive power by controlling the i_u^d and i_u^q, respectively.
- By controlling the reactive power control loop, the UIPC provides reactive power to restore the CP voltage in compliance with LVRT requirements.
- By controlling the active power control loop, the UIPC controls active power of WF injected to power system, which helps to WF stability. Also, by addition modified control system, the output power and rotor speed oscillation of nearby SGs are effectively damped.

Fig. 7 *LVRT requirements of E.ON grid code during fault*
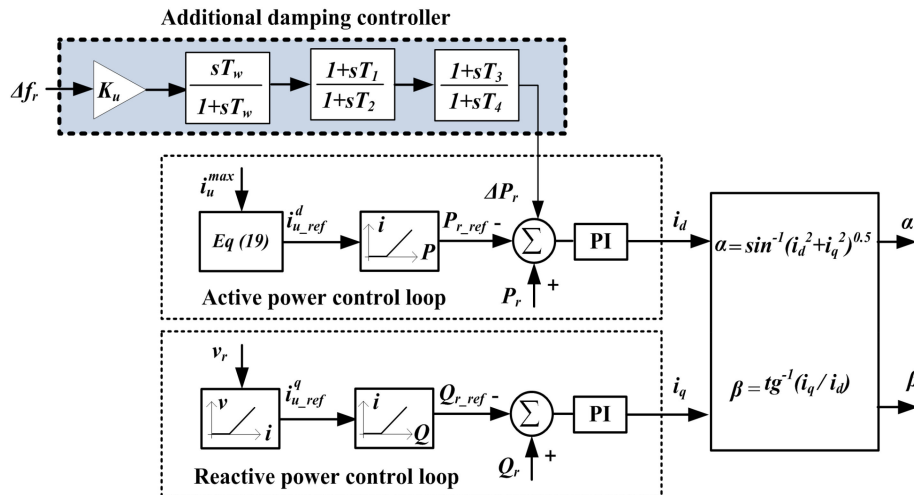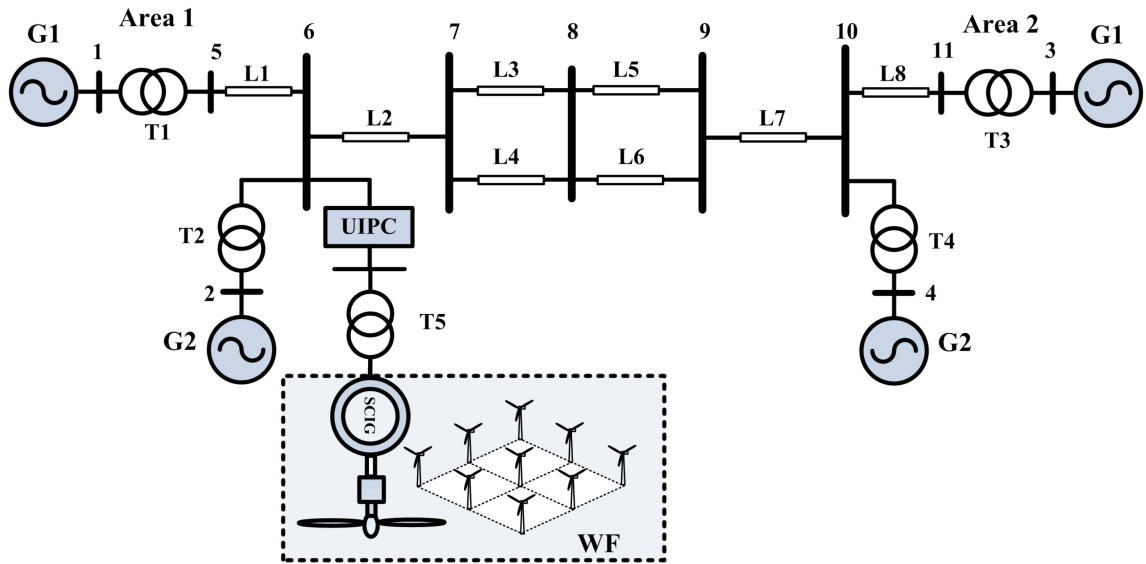*(a)* active and reactive current, *(b)* active and reactive power injected by UIPC to grid

Fig. 8 *Modified control system of SECs of the UIPC during fault operation mode*

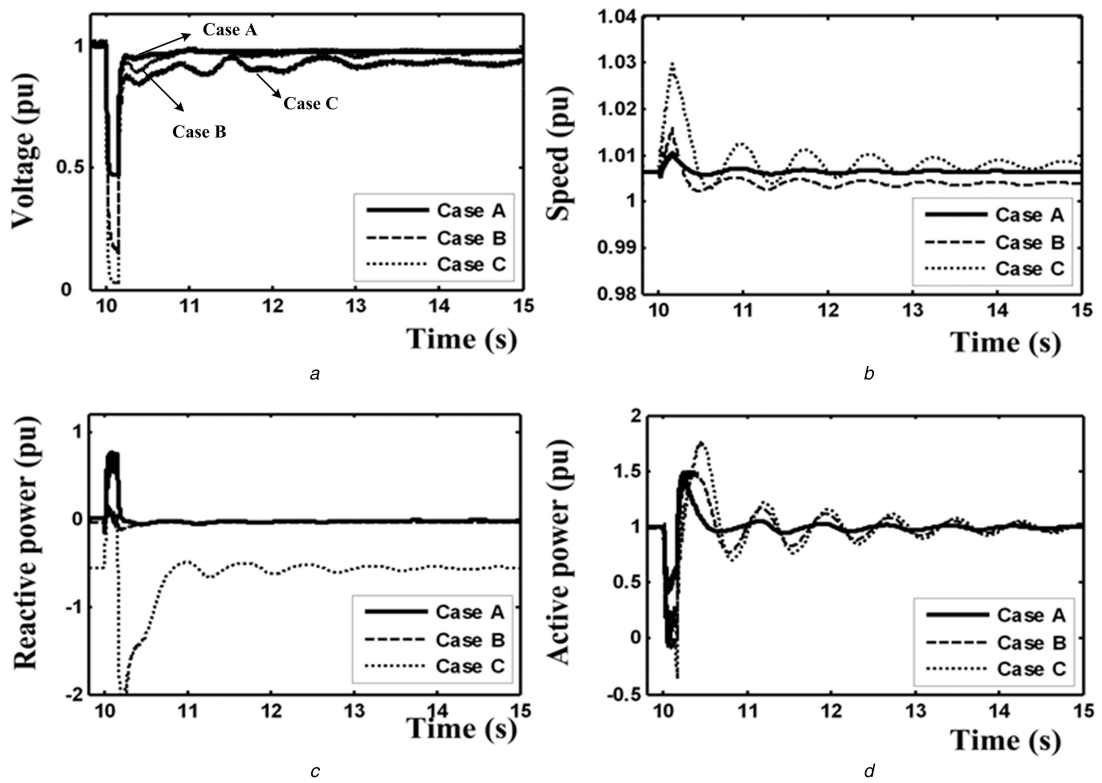**Fig. 9** *Equivalent circuit of power system under study*

Fig. 10 *Response of WF subject to three phase short-circuit fault for three cases*
(a) CP voltage of WF, *(b)* rotor speed of SCIG, *(c)* WF reactive power, *(d)* WF active power
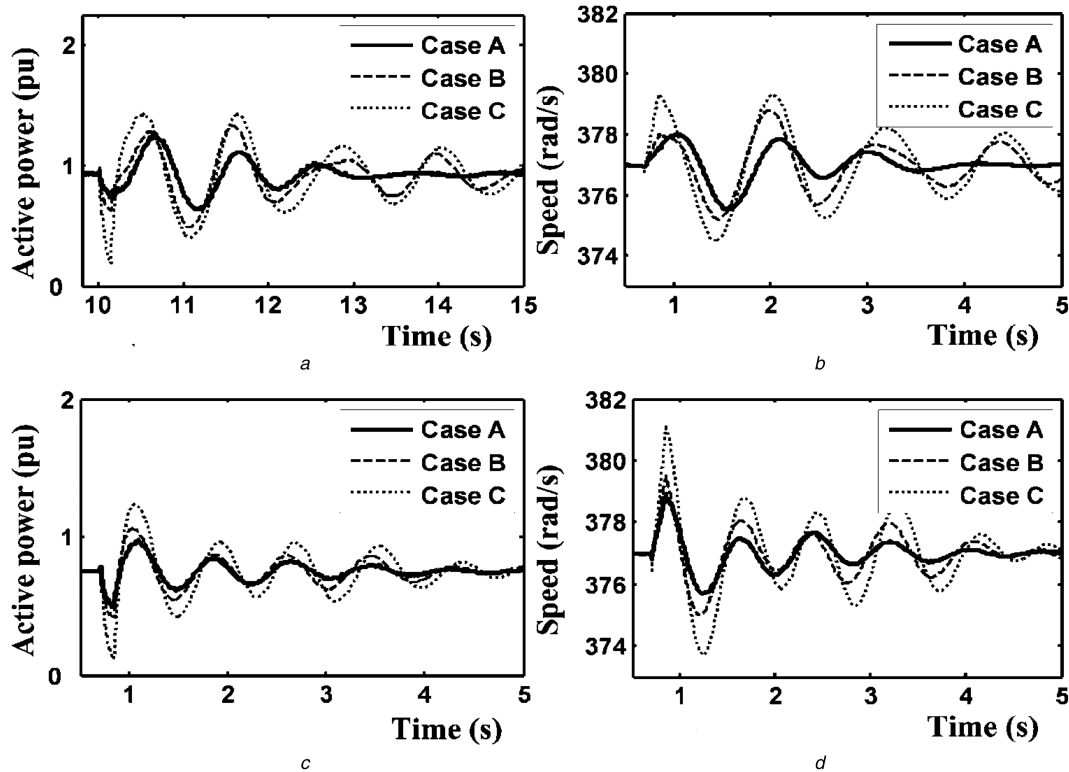
Fig. 11 *Response of power system subject to three phase short-circuit fault for three cases*
(a) Active power of G1, *(b)* rotor speed of G1, *(c)* Active power of G2 and *(d)* rotor speed of G2

6 References

[1] Liserre, M., Cardenas, R., Molinas, M*., et al.*: 'Overview of multi-MW wind turbines and wind parks', *IEEE Trans. Ind. Electron.*, 2011, **58**, (4), pp. 1081–1095

[2] Pannell, G., Atkinson, D.J., Zahawi, B.: 'Analytical study of grid-fault response of wind turbine doubly fed induction generator', *IEEE Trans. Energy Convers.*, 2010, **25**, (12), pp. 1081–1091

[3] Pedra, J., Córcoles, F., Monjo, L*., et al.*: 'On fixed-speed WT generator modeling for rotor speed stability studies', *IEEE Trans. Power Syst.*, 2012, **27**, (1), pp. 397–406

[4] Tsili, M., Papathanassiou, S.: 'A review of grid code technical requirements for wind farms', *IET Renew. Power Gener.*, 2009, **3**, (12), pp. 308–332

[5] Leon, A.E., Msuricio, J.M., Exposito, A.G*., et al.*: 'Hierarchical Wide-Area control of power system including wind farms and FACTS for short term frequency regulation', *IEEE Trans. Power Syst.*, 2012, **27**, (4), pp. 2084–2092

[6] Gounder, Y.K., Nanjundappan, D., Boominathan, V.: 'Enhancement of transient stability of distribution system with SCIG and DFIG based wind farms using STATCOM', *IET Renew. Power Gener.*, 2016, **10**, (8), pp. 1171–1180

[7] Hasanien, H.M.: 'Shuffled frog leaping algorithm-based STATCOM for transient stability improvement of a grid-connected wind farm', *IET Renew. Power Gener.*, 2014, **8**, (6), pp. 722–730

[8] Kanchanaharuthai, A., Chankong, V., Loparo, K.A.: 'Transient stability and voltage regulation in multi-machine power systems Vis-à-Vis STATCOM and battery energy storage', *IEEE Trans. Power Syst.*, 2015, **30**, (5), pp. 2404–2416

[9] Wang, L., Vo, Q.s.: 'Power flow control and stability improvement of connecting an offshore wind farm to one machine infinite bus system using a SSSC', *IEEE Trans. Sustain. Energy*, 2013, **4**, (3), pp. 358–369

[10] Leon, A.E., Farias, M.F., Battaiotto, P.E*., et al.*: 'Control strategy of a DVR to improve stability in wind farms using squirrel-cage induction generators', *IEEE Trans. Power Stabil.*, 2011, **26**, (3), pp. 1609–1617

[11] Salami, Y., Firouzi, M.: 'Dynamic performance of wind farms with bridge-type superconducting fault current limiter in distribution grid'. 2nd Int. Conf. on Electric Power and Energy Conversion Systems (EPECS), June 2011

[12] Firouzi, M., Gharehpetian, G.B.: 'Improving fault ride-through capability of fixed-speed wind turbine by using bridge-type fault current limiter', *IEEE Trans. Energy Convers.*, 2013, **28**, (2), pp. 361–369

[13] Pourhosseini, J., Gharehpetian, G.B., Fathi, S.H.: 'Unified inter-phase power controller (UIPC) modeling and its comparison with IPC and UPFC', *IEEE Trans. Power Deliv.*, 2012, **45**, (1), pp. 98–107

[14] Brochu, J., Beauregard, F., Morin, G*., et al.*: 'The IPC technology: a new approach f or substation updating with passive short circuit limitation', *IEEE Trans. Power Deliv.*, 1998, **13**, (1), pp. 233–240

[15] Brochu, J., Beauregard, F., Lemay, J*., et al.*: 'Application of the interphase power controller technology for transmission line power flow control', *IEEE Trans. Power Deliv.*, 1997, **12**, (2), pp. 888–894

[16] Fernandez, L., Garcia, C., Jurado, F.: 'Equivalent model of wind farms by using aggregated wind turbines and equivalent winds', *Energy Covers. Manag.*, 2009, **50**, pp. 691–704

[17] Murdoch, A., Winkelman, J.R., Javid, S.H*., et al.*: 'Control design and performance analysis of a 6 Mw wind turbine generator', *IEEE Trans. Power Appar. Syst.*, 1983, **PAS 102**, (5), pp. 1340–1347

[18] Anderson, P.M., Bose, A.: 'Stability simulation of wind turbine systems', *IEEE Trans. Power Appar. Syst.*, 1983, **PAS-102**, (12), pp. 3791–3795

[19] Alizadeh, M., Khodabakhshi-Javani, N., Gharehpetian, G.B*., et al.*: 'Performance analysis of distance relay in presence of unified interphase power controller and voltage-source converters-based inter phase controller', *IET Gener. Transm. Distrib.*, 2015, **9**, pp. 1642–1651

[20] Kundur, P.: '*Power system stability and control*' (McGraw-Hill, 1993)

7 Appendix

See Tables 1 and 2.

Table 1 Parameters of UIPC

Rated SEC1	25 MVA
Rated SEC2	25 MVA
Rated SHC	25 MVA
$X_L = X_C$	81.68 Ω
L	260 mH
C	38.97 µF
DC-link voltage (V_{DC})	10 kV

Table 2 Parameters of SCIG

Rated power	2 MW
Rated voltage	690 V
X_{ls}	0.1022 p.u.
X_{lr}	0.1123 p.u.
R_s	0.0074 p.u.
R'_r	0.0061 p.u.
H	5 s
X_M	4.3621 p.u.

IET Renew. Power Gener., 2017, Vol. 11 Iss. 8, pp. 1246-1252

1253